Water Practice & Technology

IWA PUBLISHING

Water Practice & Technology Vol 18 No 7, 1639 doi: 10.2166/wpt.2023.084

Geo-electrical investigation for characterizing the shallow Quaternary aquifer parameters and vulnerability to contamination: a case study from semi-arid Khanasser Valley region, Syria

Jamal Asfahani

Geology Department, Atomic Energy Commission, P.O. Box 6091, Damascus, Syria
E-mail: cscientific3@aec.org.sy

ABSTRACT

Schlumberger configuration was used to carry out 34 vertical electrical sounding (VES) measurements for estimating and characterizing the shallow Quaternary aquifer parameters and its vulnerability to surficial contamination in the region of Khanasser Valley, Northern Syria. The data of VES are interpreted by the curve matching technique (CMT) and WinResist software package to get one dimensional (1D) geoelectrical solution model for each study VES point. The electrical conductivity (EC), total dissolved solids (TDS), porosity (Ø%), the overburden protective capacity (OPC), and the corrosion (Corr) of the study aquifer were revealed by parameters of longitudinal conductance and transverse resistance of Dar-Zarrouk results. The protective capacity for the shallow Quaternary aquifer is classified as 56% poor, indicating high vulnerability to contamination, 5.9% weak, 14.7% moderate, 20.6% good, and 2.9% excellent. The ratings of corrosivity for the study region are classified as 26.5% slightly corrosive (SC), 61.8% moderately corrosive (MC), 5.9% very strongly corrosive (VSC), and 5.9% practically noncorrosive (PNC).

Key words: anisotropy, Khanasser Valley, overburden protective capacity, semi-arid regions, Syria, VES measurements

HIGHLIGHTS

- VES data are 1D interpreted to get the optimum model for each study VES point.
- Longitudinal conductance and transverse resistance are used to evaluate EC, TDS, Ø%, OPC, and Corr of the study aquifer.
- 56% of the study area has a high vulnerability to contamination, 5.9% weak, 14.7% moderate, 20.6% good, and 2.9% excellent.

GRAPHICAL ABSTRACT

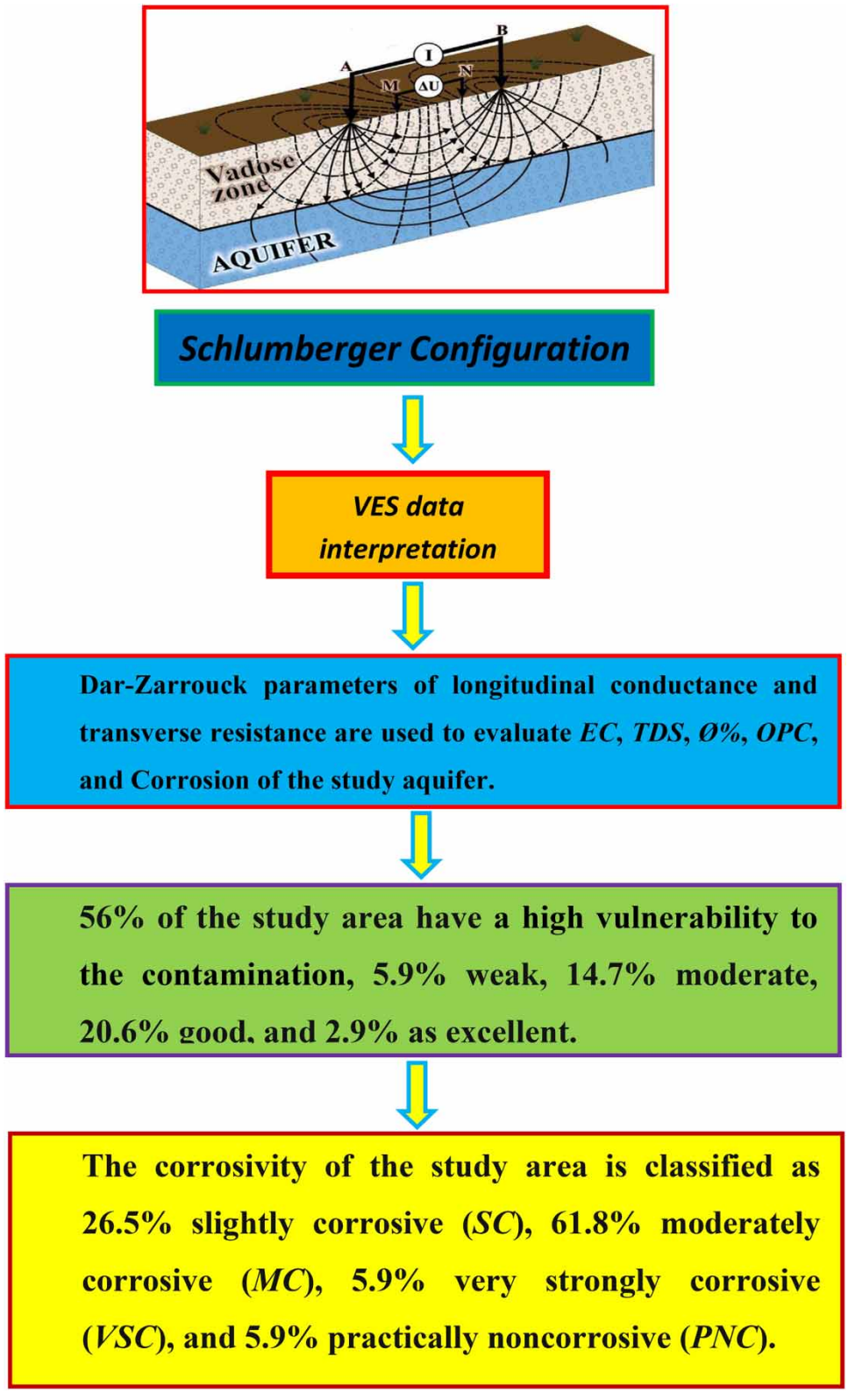

1. INTRODUCTION

Water is an important and fundamental resource to the existence of life and also the most dominant in the earth system. It exists in various forms as streams, lakes, rivers, oceans, and groundwater. The water contained beneath

the earth's surface in rocks and soil is called groundwater that is stored underground in aquifers. Groundwater is readily available as an alternative source of water for domestic, public and industrial usage, particularly in regions where there are limited surface water bodies and usually require minimum treatment to make it potable (Bayewua *et al.* 2018; Umar & Igwe 2019). The location of the groundwater in the weathered fractured rocks and soils in the pores presents many challenges for managing and quantifying the groundwater if compared with surface water. Contamination of the groundwater could pose a serious problem to the government and the people living in a given area, and can lead to diseases affecting human health. The degradation of groundwater quality could be caused by surface contaminants infiltration into the layers of the aquifer due to some environmental or geologic factors (Van Stempvoort *et al.* 2013; Obiora *et al.* 2015a, 2015b; George *et al.* 2016; Ibuot *et al.* 2017). As a result of the contamination of surface water bodies, there has been an increasing demand for groundwater to meet the world population growth (Reilly *et al.* 2008; George *et al.* 2015).

The availability of good-quality groundwater depends essentially on the permeability and porosity of the host rocks. The lithological units and the geological properties of a formation, which differ significantly from place to place, control the capacity of the hydrological unit to store groundwater.

The groundwater and electrical currents depend upon their potential gradients and are known to run from sites with higher potential to sites with lower potential. The electrical and hydraulic conductivities of an aquifer are therefore predicted to be influenced by similar variables and manner, as ions flow through water paths. The description and quantitative analysis of the aquifer units is a useful tool in both contamination migration modeling and groundwater research (Freeze & Cheery 1979; Asfahani 2007, 2013; Asfahani & Abou Zakhem 2013; George *et al.* 2015).

The cheap geoelectrical resistivity technique with its different possible applications and methodologies is widely used in groundwater exploration research, since it gives better and more rapid results in comparison with other geophysical methods (Zohdy *et al.* 1974). The resistivity which influences the artificial or natural electrical fields generated in the earth's subsurface depends on the lithology, the existence of water content, and the quality of water and pores.

The quantitative interpretation of vertical electrical sounding (VES) data constrained with logged borehole information is one of the approaches widely practiced for solving different hydrogeological and environmental problems (Oguama *et al.* 2019). Recent research demonstrates and documents the importance of using the VES technique in a hydrological domain. Hasan *et al.* (2019) applied an integrated approach including electrical resistivity with different geophysical methods to investigate the hard rock aquifers occurring in the weathered terrains of south China. They concluded that the high potential aquifers are contained within the fractured and weathered zones. Hasan *et al.* (2021) employed also VES technique in Huizhou ADS site in China to delineate the aquifer's potential zones contained within the weathered rocks. They used the available hydraulic conductivity and transmissivity data from the existing borehole pumping tests to establish empirical relationships with aquifer resistivity to be generalized on the entire study area.

De Almeida (2021) indicated the importance of applying VES technique for preliminary porous aquifer characterization, especially in the regions absent or with insufficient monitoring wells.

Akingboye *et al.* (2022) demonstrated the advantages of integrating different geophysical techniques to investigate the near-surface crustal architecture and geohydrodynamics of the crystalline basement terrain of Araromi, Southwestern Nigeria. Akingboye (2022) applied the VES technique with the Schlumberger array to assess the groundwater yield of aquifer units and their vulnerability to contaminants in Araromi, Southwestern Nigeria. Ikpe *et al.* (2022) applied VES to assess the protectivity of hydrogeological units in Ikot Ekpene Urban and its environs in Southern Nigeria, where valuable information has been provided to design effective groundwater and waste disposal management in the study area.

Aretouyap *et al.* (2022) used the VES technique with the contribution of the fuzzy algebraic model to the sustainable management of groundwater resources in the Adamawa watershed, where *new hydrological insights* combining six hydro-parameters contributing to groundwater occurrence in a GIS environment are discussed and documented to assess the groundwater potential (GWP) in the study region.

Abdulrazzaq *et al.* (2023) used also the VES technique to determine the optimum drilling sites for groundwater wells based on the hydro-geoelectrical parameters and weighted overlay approach via GIS in the Salah Al-Din area, central Iraq.

Given the above, this paper simulates the recent hydrogeological trends and therefore employs the VES and regression modeling techniques to determine and predict the spatial variations of the different aquifer parameters and groundwater quality in shallow Quaternary aquifers in the Khanasser region, Northern Syria.

This research work is part of an international integrated program for geophysical research, realized in the Valley of Khanasser, with the collaboration of three scientific organizations; Syrian Atomic Energy Commission (SAEC), International Center for Agriculture Research in the Dry Areas (ICARDA) and Bonne University, Germany. Figure 1 shows the location of the region of Khanasser Valley in Syria. The aim of this international program was originally since its beginning to resolve different problems related to peripheral dry-land environments. The relatively easy accessibility, dynamics and diversity of the natural resources, livelihoods, and poverty made Khanasser a prime candidate.

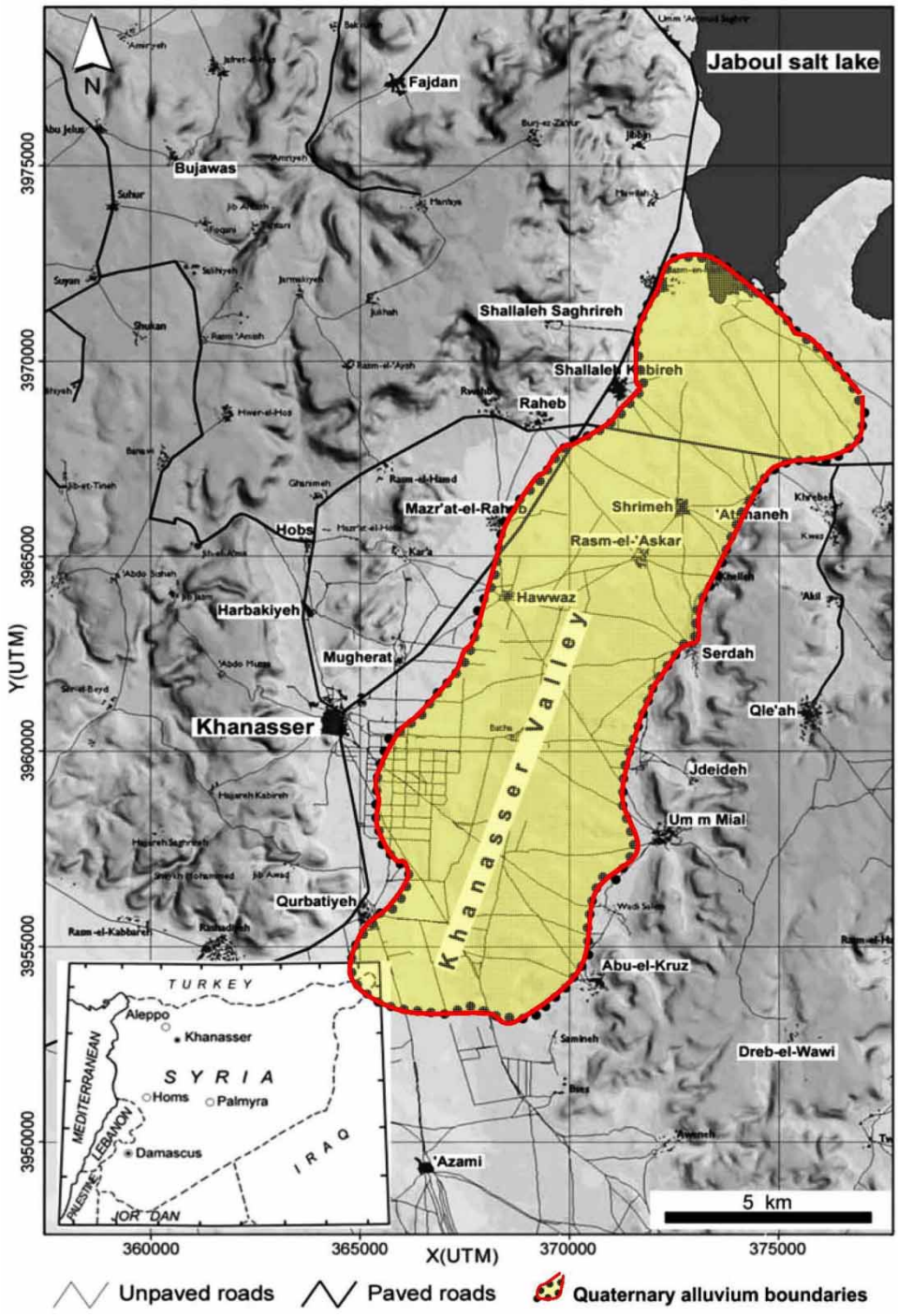

Figure 1 | Location of the Khanasser Valley, Northern Syria.

The original news in the paper is to characterize the shallow Quaternary aquifer in the Khanasser Valley area by using the regression analysis modeling technique and developing the Dar-Zarrouk parameters (DZPs), resulting from interpreting the VES datasets. Those (DZP) allow us to predict the water resistivities even in locations

where no samples of water are available. The first new predicting procedure developed in this paper permits consequently to characterize the parameters of *electrical conductivity* (EC), *total dissolved solids (*TDS*), formation factor* (*F*), and *porosity* (*Φ*%) of the Quaternary aquifer, and follow their spatial variations in the study region. The second new aspect in this research paper is an attempt to characterize the aquifer's vulnerability to contamination and corrosion by adopting a specific methodology approach, aimed at evaluating and identifying both the overburden protective capacity (OPC) and the corrosion of the aquifer (Corr). This new aspect, highly important for both industry and the environment is applied for the first time in Syria. The environmental topic of this paper is oriented therefore toward achieving and determining safe drinking water locations in accordance with sustainable development goals (SDGs).

The main objectives of this paper are therefore to determine and estimate the geoelectrical characteristics of the subsurface lithological units in the Khanasser Valley area by applying an integrated VES methodology approach. This application is to get information about the subsurface layer descriptions and the vulnerability of the shallow Quaternary aquifer to contamination as follows:

- Characterizing the subsurface geoelectrical layers through interpreting 34 VES data points, and their related DZP of total resistance (TR), transverse resistivity (ρ_t), total conductance (S), longitudinal resistivity (ρ_l), and anisotropy (λ).
- Establishing a calibrated equation line between transverse resistance (TR) related specifically to the shallow Quaternary aquifer and modified transverse resistance (MTR). This calibration line allows us to extrapolate and deduce the values of water resistivity samples in the VES points, where water samples do not exist. The EC, TDS, *F*, and *Ø*% are consequently derived for the shallow Quaternary aquifer in the study area.
- Determining the corrosion (Corr) and the vulnerability to contamination through analyzing the longitudinal conductance (Ω^{-1}) and shallow aquifer overburden capacity protection (OPC).
- Mapping the different hydrogeophysical parameters related to the shallow Quaternary aquifer (EC, TDS, *F,Φ,* TR, *S,* ρ_t, ρ_l, λ, OPC, and Corr) in the study Khanasser Valley region.

2. HYDROGEOLOGY OF THE KHANASSER VALLEY

Khanasser Valley is nearly 70 km southeast of Aleppo City, and is located between two hill series; the Jabal Al Hoss in the west, and Jabal Shbeith in the east as seen in Figure 1. The drain of the southern and northern parts of the valley is toward the Adami depression and the Jaboul salt lake, respectively, as seen in Figures 1 and 2.

The groundwater extraction in the Khanasser Valley is carried out through three existing aquifers. The deepest aquifer is the upper Cretaceous, 400 m below the ground level. The second aquifer of Paleocene-Lower Eocene limestone is located above the Maestrichtian and is of low productivity (ACSAD 1984). The average hydraulic conductivity (k) of this aquifer is equal to 0.0054 m/day (Schweers *et al.* 2002). In the central part of the Khanasser Valley, the paleogene strata of around 50 m of Paleocene and lower Eocene is not too thick over the Maestrichtian formation.

Figure 2(a) shows a geological cross-section along the AB profile indicated in Figure 2.

3. VERTICAL ELECTRICAL SOUNDINGS TECHNIQUE

In total, 34 vertical electrical soundings (VES) disseminated on three longitudinal profiles (LP1, LP2, and LP3) were performed across the Khanasser Valley study area, with the use of the Schlumberger electrode configuration shown in Figure 2(b).

The geology of the study region and the positions of those VES points are shown in Figure 2(a). The coordinates of the VES points were recorded with the global positioning system (GPS). The electrical resistivity survey was performed using a resistivity meter with its accessories (Indian one, ACR1 unit), that enabled measuring of the apparent resistance of the subsurface through injecting electrical current into the earth and receiving potential at the surface. The transmitting and receiving electrodes were the current (A and B) and potential electrodes (M and N), respectively. The half-current electrode spacing AB/2 was ranged from 3.0 to 500 m and the half-potential electrode spacing *MN/2* were ranged from 0.25 to 20 m. The apparent resistivity (ρa) for the Schlumberger electrode array configuration is determined through the following equation:

$$\rho_a = \frac{2\pi}{(1/\mathrm{AM}) - (1/\mathrm{BM}) - (1/\mathrm{AN}) + (1/\mathrm{BN})}\frac{\Delta V}{I} \quad (1)$$

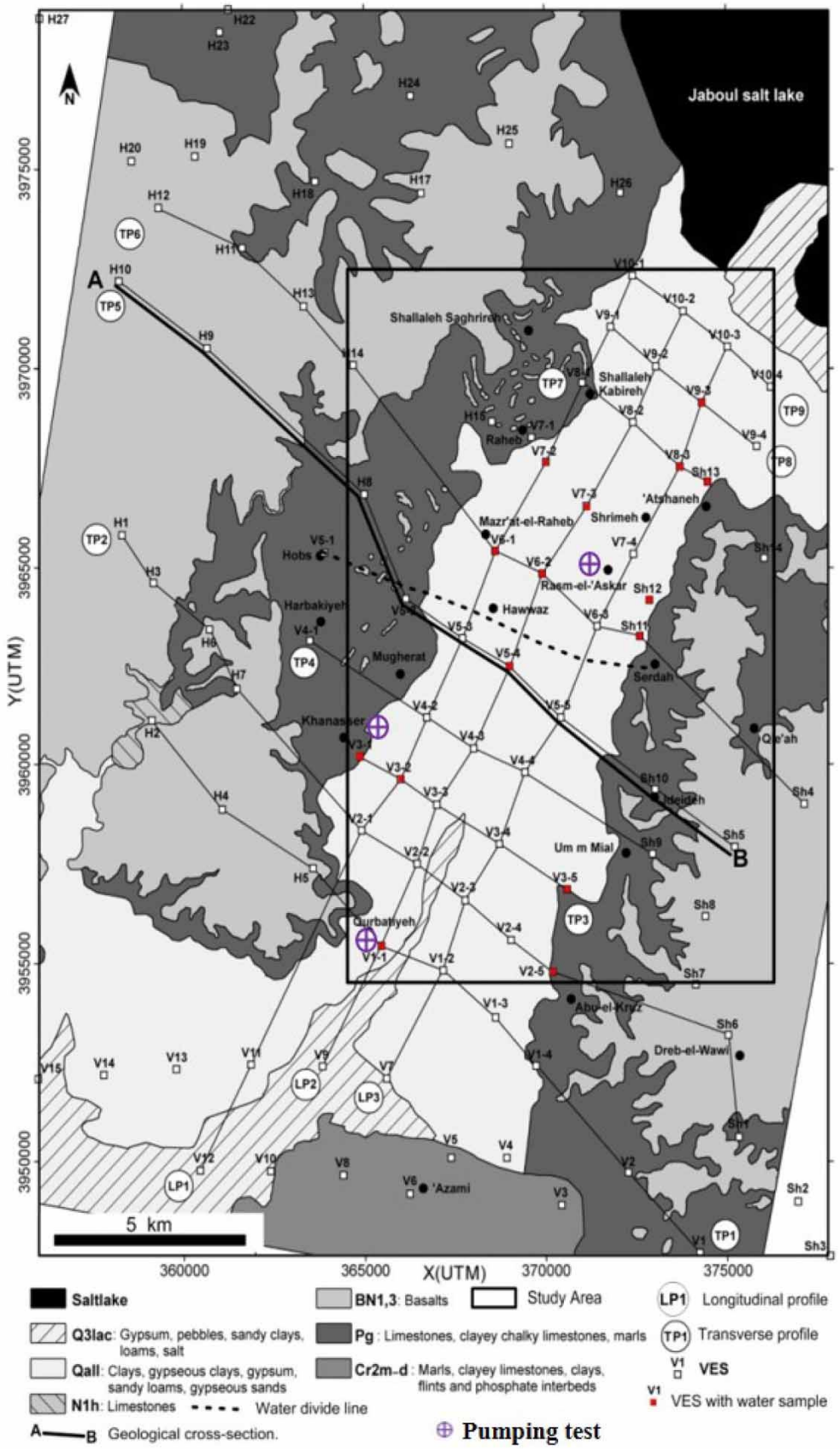

Figure 2 | Geological map of the Khanasser Valley and its surroundings (After Ponikarov 1964), with the locations of VES soundings (Asfahani 2016). (a) Geological cross-section along the AB profile (Asfahani 2013). (b) Schlumberger configuration in the field. (*continued*.).

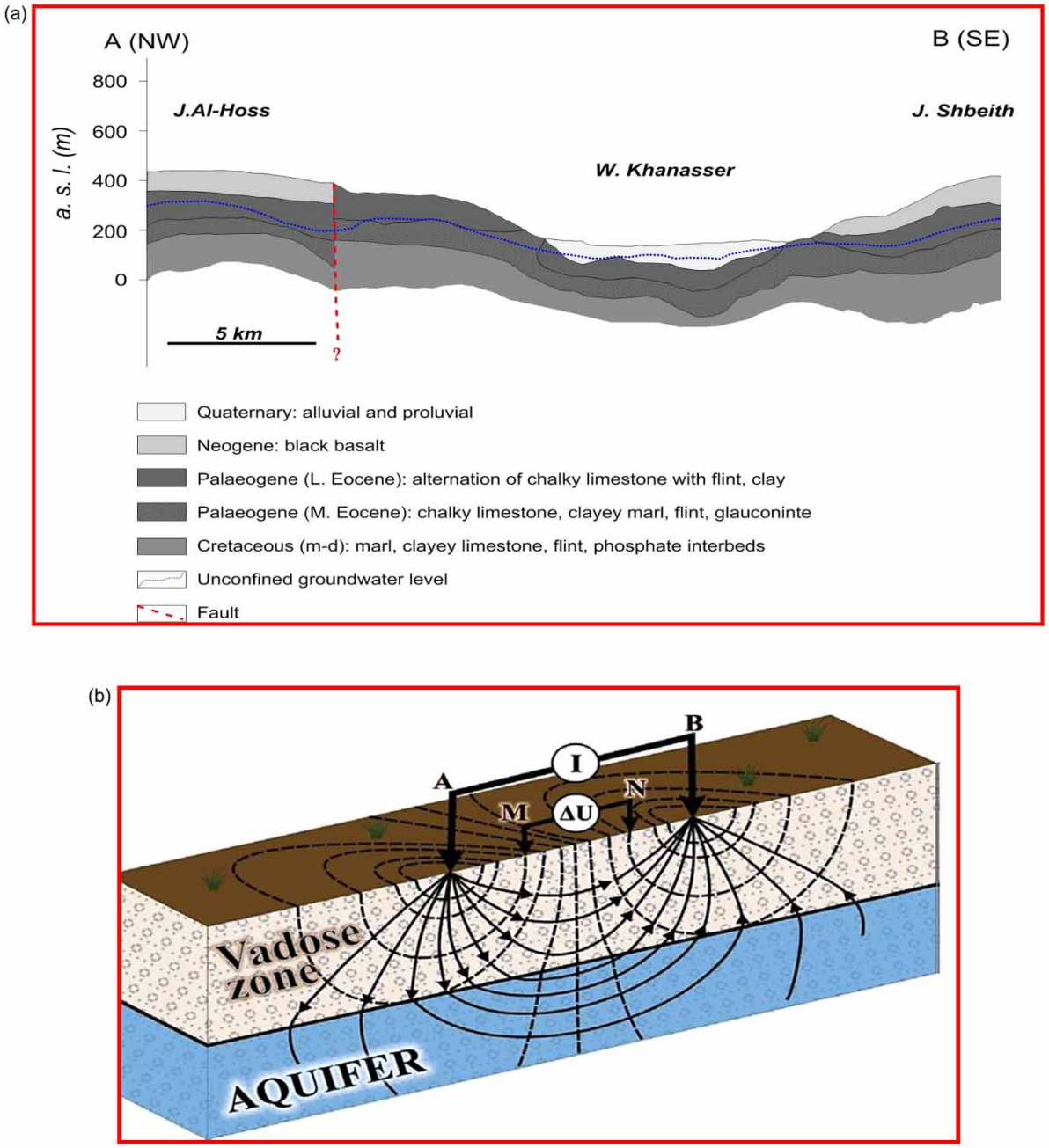

Figure 2 | Continued.

where I is the current injected into the ground, and ΔV is the potential measured at the surface. Equation (1) was used to compute the apparent resistivity, where the resistance $\Delta V/I$ is directly measured.

The complete field apparent resistivity curve is obtained by increasing the electrode spacing $AB/2$ about a fixed point. Conventional manual curves (CMC) and auxiliary charts were used to smooth this field apparent resistivity curve to eliminate the effects of lateral inhomogeneities, and to quantitatively interpret it in terms of true resistivity and thickness (Orellana & Mooney 1966; Zohdy *et al.* 1974). To improve upon the initial manually interpreted VES data, the initial parameters of the approximate model are thereafter interpreted by an inversion WINRESIST software of Velpen (2004) to accurately get the final optimum model, in which a good fit between the final theoretical regenerated curve and the field apparent resistivity curve was obtained (Zohdy 1989; Zohdy & Bisdorf 1989). The final optimum model includes the values of real resistivity, depth, and thickness of each geoelectrical layer. Both layer resistivity (ρ) and thickness (h) are two fundamental parameters for understanding and interpreting the geoelectrical models for characterizing and describing the subsurface hydrogeological units under each studied VES.

4. METHODOLOGY APPROACH

The methodology approach applied in this research consists of two parts. The first part characterizes the shallow Quaternary aquifer in the study Khanasser Valley area, by determining the spatial variations of EC, TDS, *F*, and Ø%.

The second part evaluates the OPC of the Quaternary aquifer, and the corrosion (Corr) parameter in the study region.

This methodology approach in its two parts is based essentially on the second geoelectrical indices of DZP as described below.

4.1. Hydro-geoelectrical model and DZP

The fundamental parameters describing the geoelectrical layers are derived from the quantitative interpretation of the VES datasets, as the real resistivity (ρ_i) and thickness (h_i) values along the study area; where the subscript '*i*' refers to the layer position in the geoelectrical section. Some geoelectrical parameters can be also derived from these basic resistivity and thickness parameters, such as the total longitudinal conductance (*S*) and total transverse resistance (TR). These have been illustrated as the DZP (Maillet 1974; Oladapo & Akintorinwa 2007; Asfahani 2016; IKpe *et al.* 2022).

A unit square cross-section area cut out of a group of n-layers of infinite lateral extent is taken into consideration in order to obtain the hydro-geoelectrical parameters as follows:

The total transverse unit resistance TR is given by the following equation:

$$\mathrm{TR} = \sum_{i=1}^{n} h_i \rho_i \tag{2}$$

The total longitudinal conductance *S* is given by the equation:

$$S = \sum_{i=1}^{n} \frac{h_i}{\rho_i} \tag{3}$$

where h_i and ρ_i are the layer thickness and resistivity of *i*th layer in the section, respectively.

TR and *S* are called the DZP, that allow us to get the transverse resistivity (ρ_t) and longitudinal resistivity (ρ_l), respectively, as expressed by Equations (4) and (5).

$$\rho_t(\Omega m) = \frac{\sum_{i=1}^{n} h_i * \rho_i}{\sum_{i=1}^{n} h_i} \tag{4}$$

$$\rho_l(\Omega \mathrm{m}) = \frac{\sum_{i=1}^{n} h_i}{\sum_{i=1}^{n} (h_i/\rho_i)} \tag{5}$$

Zohdy *et al.* (1974) have shown that DZPs are a powerful tool for groundwater exploration surveys.

Generally, the longitudinal resistivity (ρ_l) is less than the transverse resistivity (ρ_t) unless the medium is uniform (Flathe 1955). Keller (1987) also suggested that the more conductive layers dominate the distribution of (ρ_l) (the clay and weathered/sediments dominate in the present case study, even if a small fraction of resistive layers is present).

The combination of Equations (4) and (5) allows us to obtain the anisotropy parameter (λ) as expressed by Equation (6):

$$\lambda = \sqrt{\frac{\rho t}{\rho l}} \tag{6}$$

The DZPs are developed in the present paper in order to characterize as precisely as possible the shallow Quaternary aquifer and its vulnerability to contamination in the Khanasser Valley, Northern Syria. In fact, those parameters help in interpreting and analyzing the structural characteristics and subsurface lithology with reduced uncertainties (Maillet 1974). In addition, the anisotropy parameter plays an important role in aquifer vulnerability and groundwater assessment.

4.2. EC, TDS, *F*, and Ø% determination

Fifteen VES measurements (from the total of 34 VES) were carried out close to the water sample locations, and have been quantitatively interpreted. An empirical calibrated relationship is established in this paper for those 15 VES points between the Dar-Zarrouk transverse resistance TR (TR is the product of the saturated aquifer thickness h and its resistivity ρ_e) and the parameter of MTR. MTR takes into account the ratio of the resistivity of the water sample and the average of those resistivities for the available 15 VES points (3.35 Ω m) (Asfahani 2016) as follows:

$$\mathrm{MTR} = \frac{3.35}{\rho_w} * \mathrm{TR} \tag{7}$$

The relationship between MTR and TR has the following form:

$$\mathrm{MTR} = 0.20 * \mathrm{TR}^{1.33} \quad \text{with } (R^2 = 0.77) \tag{8}$$

This calibration equation line is used thereafter to predict and extrapolate the values of the resistivity water samples ρ_w (Ω.m) in the 19 VES points, where no samples of water are available by using the following equation:

$$\rho w_i = \bar{\rho_w} * \frac{\mathrm{TR}_i}{\mathrm{MTR}_i} \tag{9}$$

In which $\bar{\rho w}$ is the average water resistivity value of the available 15 water samples (3.35 Ω m), and $(\rho_w)_i$ is the water resistivity at the location of the $(\mathrm{VES})_i$ point.

The EC and the TDS of the shallow Quaternary aquifer can be thereafter obtained by using the following relationships:

$$\mathrm{EC(dS/m)} = \frac{1}{\rho_w} \tag{10}$$

$$\mathrm{TDS(ppm)} = 640 * \mathrm{EC(dS/m)} \tag{11}$$

The F used in Archie's law 1942 in its general form is calculated as the ratio of ρ_e and ρ_w as follows:

$$F = \frac{\rho_e}{\rho_w} \tag{12}$$

The Ø% of the Quaternary aquifer in the study Khanasser area is also computed using Archie's law (Archie 1942) as follows:

$$\phi(\%) = \left(\frac{a\rho_w}{\rho_e}\right)^{\frac{1}{m}} \tag{13}$$

In which ρ_e is the saturated Quaternary aquifer resistivity estimated from the quantitative interpretation of (VES), and ρ_w is the pore fluid resistivity.

The dimensionless coefficients a and m depend on the rock type.

The values of $a = 0.88$ and $m = 1.37$ were taken in this study following the values given by Keller (1988) for sands, sandstone, and some limestone (Asfahani 2007).

4.3. Protective capacity and corrosivity

The OPC of an aquifer is defined as the ratio of the overburden thickness to its resistivity (Omoyoloy *et al.* 2008). The greater the protective capacity the greater the overburden longitudinal conductance (Ω^{-1}).

DZPs resulting from the quantitative interpretation of VES soundings are used herein to evaluate the shallow Quaternary aquifer protective capacity, and longitudinal conductance of overburden units in the Khanasser Valley region. The identification of the groundwater areas vulnerable to contamination or could be contaminated by leaching is an important factor in subsurface exploration hydrogeology. The groundwater contamination

depends on porosity, permeability, and the overburden thickness of the geological layers. The unconsolidated and un-compacted coarse sand is an example of underlying material that helps and favorites the capability of polluting influents to infiltrate and escape into the subsurface to contaminate the groundwater, form a polluting plume extending hundreds of meters, and render the soil corrosive (Keswick *et al.* 1982).

A leakage, rupture pipeline, or failure pipeline could create serious hazards to the assets, environment, and even humans due to the leakage and explosion (Yahaya *et al.* 2009). The environment impacts can be easily evaluated by using geoelectrical techniques without interfering with the hydrogeologic system (Mogaji *et al.* 2007).

Henriet (1976) explained that the combination of aquifer layer thickness and resistivity using DZPs of transverse resistance and longitudinal conductance may be of a direct application in aquifer protection research, where hydrological properties of aquifers and also the protective capacity of clayey aquifer overburden can be evaluated. The longitudinal conductance (DZP) is used in this paper as a criterion for determining the shallow Quaternary aquifer protective capacity rating according to the rating shown in Table 1.

Table 1 | Longitudinal conductance/protective capacity rating (Henriet 1976; Oladapo *et al.* 2004)

Longitudinal conductance (mhos)	Protective capacity rating
>10.00	Excellent
5.00–10.00	Very good
0.70–4.90	Good
0.20–0.69	Moderate
0.10–0.19	Weak
<0.10	Poor

Soil corrosivity (Corr) is estimated by taking into consideration the resistivity value of the first layer for each VES location in the study region, and by refereeing and comparing with the corrosivity rating indicated in Table 2.

Table 2 | Classification of soil resistivity in terms of corrosivity (Baeckman & Schwenk 1975; Agunloye 1984; Oladapo *et al.* 2004)

Soil resistivity (Ω m)	Soil corrosivity
<10.00	Very strongly corrosive (VSC)
10.00–60.00	Moderately corrosive (MC)
60.00–180.00	Slightly corrosive (SC)
≥180.00	Practically noncorrosive (PNC)

The earth's medium acts as a natural filter for the percolation of fluid. The ability of the earth to accelerate or retard and filter fluid percolation is a measured parameter of its protective capacity (Barker *et al.* 2001). The zones of poor and weak protective capacity are those vulnerable to surface contaminant materials. The appreciable overburden thickness with clayey columns, which are thick enough to represent the moderate to good protective capacity zones. Those overburden layers protect the shallow aquifer in the study area from surface polluting fluid.

5. RESULTS AND DISCUSSION

Thirty-four VES points were measured in the Khanasser Valley region, Northern Syria by using Schlumberger configuration. The quantitative interpretations in terms of 1D structure of those 34 VES measurements allow us to obtain the real thicknesses and resistivities of the corresponding layers. The non-uniformity of the research area creates different geoelectrical layered models of 3–6 layers, represented by different geoelectrical curves. The

VES curve types include QH (32%), HH (26%), KHKH (5.88%), H (8.82%), KH (5.88%), HK (5.88%), HAK (5.88%), HKH (2.94%), QHKH (2.94%), and QQH (2.94%) as represented by Figure 3.

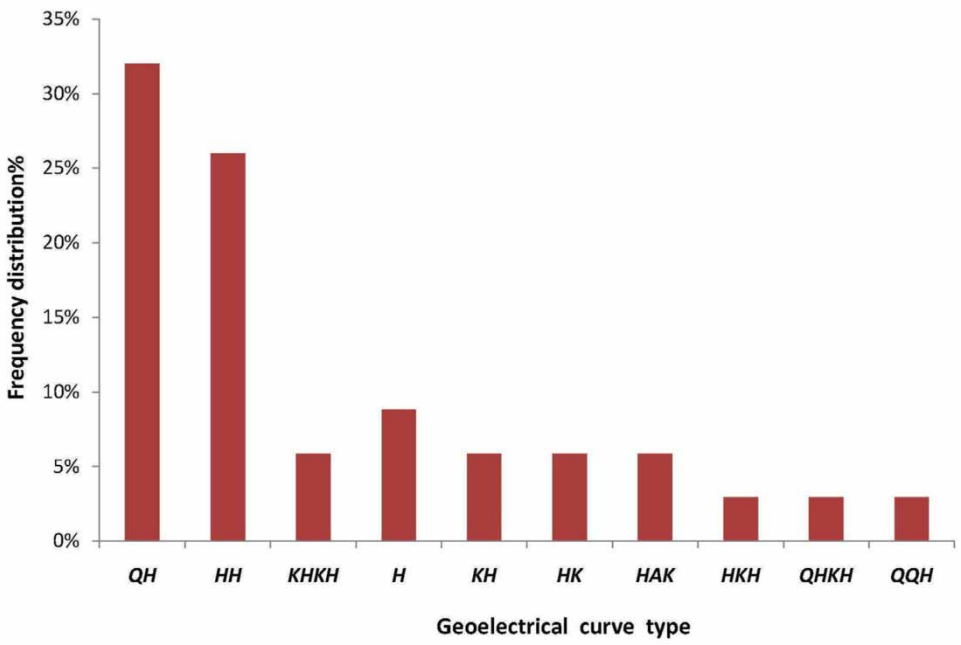

Figure 3 | Frequency distribution of the geoelectrical curve types in the Khanasser Valley region.

Figure 4 shows 1D quantitative interpretation of VES at point V2-3 of QQH geoelectrical curve type, with the comparison with the available lithological description of well No. 1, located closely to this V2-3 point. The two top first layers are represented by an equivalent one layer of resistivity of 120 Ω m and a thickness of 5.4 m (Figure 4(c)). The alluvial gravels and sand, known as rammel aswad in the study area according to the farmers in the region are responsible for the shallow Quaternary aquifer transmissivity, where its high thickness offers high yields and transmissivity. This rammel aswad changes brutally from one place to another laterally and vertically, which explains the sharp change in the well's productivity, even in very short distances (Asfahani 2016).

The 15 VES measurements (from the total of 34 VES) close to the water sample locations are 1D quantitatively interpreted as described above, where the resulting real resistivity and thickness of the saturated shallow Quaternary aquifer (ρ_e and h) are indicated in Table 3. The empirical calibrated relationship established in this paper between the Dar-Zarrouk transverse resistance TR and the MTR established according to Equation (8) for those 15 VES points is shown in Figure 5.

This calibration equation line is used thereafter to predict and extrapolate the values of the resistivity water samples ρ_w (Ω.m) in the 19 VES points, where no water samples are available, as shown and indicated in Table 4.

The conjoint VES data (15 + 19) presented in Tables 3 and 4 will be used to characterize the spatial variations of the treated parameters for the entire Quaternary aquifer in the study area.

Table 5 shows the DZPs of TR, S, ρ_t, ρ_l, and λ computed according to Equations (2), (3), (4), (5) and (6), respectively, for the 34 VES points in the Khanasser Valley region.

The longitudinal conductance S (Ω^{-1}) varies between a minimum of 8.16 Ω^{-1} at *Sh13* and a maximum of 97.7 Ω^{-1} at V10-2, with an average of 46.4 Ω^{-1} and a standard deviation of 22.8 Ω^{-1}, where the spatial variations of S are indicated by Figure 6(a).

The longitudinal resistivity ρ_l varies between a minimum of 1.86 Ω m at V2-4 and a maximum of 15.7 Ω m at Sh13, with an average of 5.68 Ω m and a standard deviation of 3 Ω m as indicated by Figure 6(b).

The transverse resistance TR ($\Omega \cdot m^2$) varies between a minimum of 459 $\Omega \cdot m^2$ at V2-4 and a maximum of 9,123.6 $\Omega \cdot m^2$ at V2-5, with an average of 1,837.8 $\Omega \cdot m^2$ and a standard deviation of 1,495 $\Omega \cdot m^2$ (Figure 7(a)).

The transverse resistivity ρ_t varies between a minimum of 2.94 $\Omega \cdot m$ at V2-4 and a maximum of 25.5 $\Omega \cdot m$ at V2-5, with an average of 8.41 $\Omega \cdot m$ and a standard deviation of 4.9 $\Omega \cdot m$ as indicated by Figure 7(b).

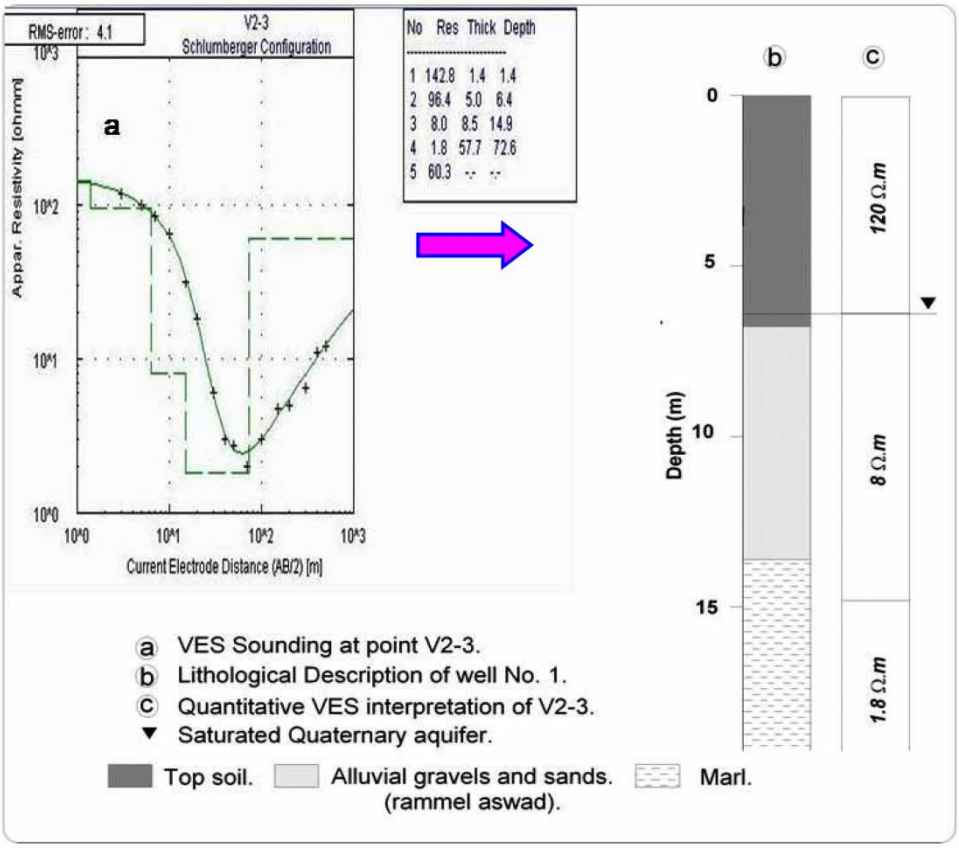

Figure 4 | Quantitative VES interpretation of V2-3 point.

The anisotropy coefficient λ varies between a minimum of 0.72 at V7-3 and a maximum of 2.31 at V2-3, with an average of 1.24, and a standard deviation of 0.29, as indicated by Figure 8, that shows the spatial variations of λ coefficient.

The sedimentological nature of the Quaternary aquifer composed of unconsolidated materials such as alluvial, proluvial, and lacustrine deposits provokes such high anisotropy values of λ (Asfahani 2013). The anisotropy results reported in this paper are in good agreement with those obtained by azimuthal VES configuration already applied for studying four VES points (V2-3, V8-2, V10-2, and V6-3) in the Khanaser valley (Asfahani 2013).

Figure 9(a) shows the cross plot between the anisotropy (λ) and the transmissivity (T) of the Quaternary aquifer determined by Asfahani (2016, 2021). One can notice the presence of three positive trends between λ *and* T, reflecting different hydraulic systems in the study Khanasser region.

Figure 9(b) shows the cross plot between the anisotropy (λ) and the transverse resistance (TR) of the Quaternary aquifer. One can notice again the presence of three positive trends between λ and TR, reflecting different hydraulic systems in the study Khanasser region.

The distribution of the EC of the Quaternary aquifer in the study Khanasser Valley obtained by integrating the 34 VES points (Tables 3 and 4) is shown in Figure 10(a). EC varies between a minimum of 1.3 dS/m at VES location of Sh12 and a maximum of 10 dS/m at the VES location V6-2 with an average of 4.1 dS/m and a standard deviation of 1.9 dS/m.

The distribution of the TDS of the Quaternary aquifer in the study Khanasser Valley obtained by integrating the 34 VES points (Tables 3 and 4) is shown in Figure 10(b).

TDS varies between a minimum of 860 ppm at the VES location *Sh12* and a maximum of 6,400 ppm at the VES location, V6-2 with an average of 2,592 ppm and a standard deviation of 1,208 ppm.

Asfahani (2007) has already developed different empirical relationships between earth resistivity, water resistivity and the available TDS *data* to predict and derive the apparent salinity TDS of only 19 VES points in the study region for different AB/2 of 70, 100, and 150 m (Figure 8). While the established TDS values in this paper are real and more accurate than previously for the following reasons:

Table 3 | Hydro-geophysical parameters of the studied 15 VES points, where water samples are available

Location	*E* (UTM)	*N* (UTM)	*h (m)*	ρ_e (Ω m)	ρ_w (Ω m)	TR (Ω.m^2)	MTR (Ω.m^2)	EC (dS/m)	TDS (ppm)	*F*	Ø (%)	OPC (Ω^{-1})	Corr
V6-1	368600	3965400	12.00	8.50	3.03	102.00	112.77	3.30	2,112.21	2.80	22.90	0.14	26.80
V9-3	374300	3969100	22.50	11.00	1.30	247.50	637.78	7.69	4,923.08	8.46	7.59	0.04	87.60
V2-5	370174	3954786	23.80	9.60	2.16	228.48	354.35	4.63	2,962.96	4.44	14.45	0.01	910.00
V1-1	365444	3955447	31.40	6.50	1.79	204.10	381.97	5.59	3,575.42	3.63	17.69	2.48	51.2.00
Sh11	372582	3963240	31.90	30.00	2.51	957.00	1,277.27	3.98	2,549.80	11.95	5.37	3.26	30.00
Sh12	372849	3964169	25.00	15.50	7.44	387.50	174.47	1.34	860.21	2.08	30.83	4.57	18.80
Sh13	374453	3967107	10.00	9.00	4.52	90.00	66.70	2.21	1,415.93	1.99	32.26	0.03	36.70
V8-3	373700	3967500	11.50	17.00	3.47	195.50	188.75	2.88	1,844.38	4.90	13.11	0.05	66.50
V3-1	364871	3960189	7.70	10.00	6.85	77.00	37.66	1.46	934.31	1.46	44.00	0.09	19.00
*V*3-2	365981	3959628	25.00	15.00	6.02	375.00	208.68	1.66	1,063.12	2.49	25.78	0.60	35.80
V7-2	370000	3967600	6.00	16.00	4.33	96.00	74.27	2.31	1,478.06	3.69	17.38	0.37	16.00
V7-3	371100	3966500	5.70	16.00	3.03	91.20	100.83	3.30	2,112.21	5.28	12.16	0.37	15.40
V3-5	370578	3956847	12.90	19.00	1.67	245.10	491.67	5.99	3,832.33	11.38	5.64	0.06	870
V5-4	369000	3962500	59.00	14.00	1.20	826.00	2,305.92	8.33	5,333.33	11.67	5.50	0.05	74.40
V6-2	369900	3964800	17.20	23.00	1.00	395.60	1,325.26	10.00	6,400.00	23.00	2.79	0.76	22.60

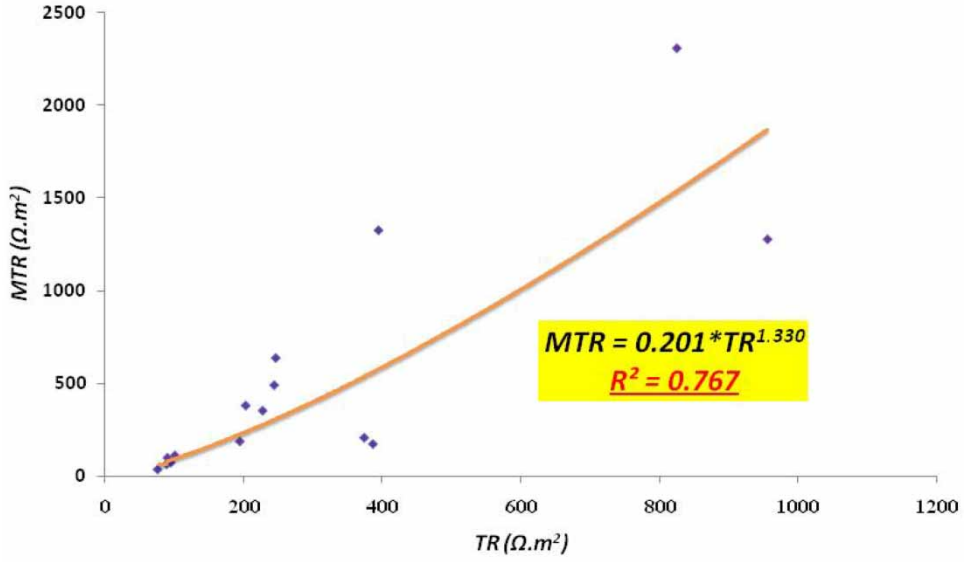

Figure 5 | Calibrated equation line between TR and MTR for 15 VES with available 15 water samples.

1. They are based on using 34 VES data points (19 + 15) according to the methodology developed and described in this paper, with the use of basically Dar-Zarrouck parameters.
2. The real resistivity and thickness of the 34 VES data points related to the Quaternary aquifer are taken into consideration while deriving the *real* TDS values.

The distribution of the *F* of the Quaternary aquifer in the study Khanasser Valley obtained by integrating the 34 VES points (Tables 3 and 4) is shown in Figure 11(a). *F* varies between a minimum of 1.5 at the VES location V2-2 and a maximum of 23 at the VES location V6-2, with an average of 6.5 and a standard deviation of 5.4.

The distribution of the *Ø*% of the Quaternary aquifer in the study Khanasser Valley obtained by integrating the 34 VES points (Tables 3 and 4) is shown in Figure 11(b). *Ø*% varies between a minimum of 2.8% at the VES location V6-2 and a maximum of 44% at the VES location V3-1, with an average of 16.9% and a standard deviation of 11.8%.

Table 6 summarizes the geoelectrical and hydrological parameters obtained through studying and analyzing 34 VES points for characterizing the Quaternary aquifer in the Khanasser Valley, Syria.

The OPC of the shallow Quaternary aquifer is classified according to Tables 1, 3 and 4 as 56% poor, indicating high vulnerability to contamination in the VES locations of *V9-3, V2-5, Sh13, V8-3, V3-1, V3-5, V5-4, V10-4, V10-1, V9-1, V9-4, V8-2, V5-3, V5-5, V4-3, V3-3, V2-3, V2-4,* and V1-2, 5.9% weak in the VES locations of V6-1 and V3-4, 14.7% moderate in the VES locations of V3-2, V7-2, V7-3, V9-2, V2-1, and *V2-2*, 20.6% good in the VES locations of V1-1, Sh11, Sh12, V6-2, V10-3, and V6-3, and 2.9% as excellent in the VES locations of V10-4.

The percolation of the fluid is originated from the earth's medium that acts as a natural filter. The OPC is the measure of the earth's ability to accelerate or retard and filter fluid percolation (Barker *et al.* 2001).

Figure 12 shows the spatial variation of the OPC in the study area.

The Quaternary aquifer in the study area is protected from the surface polluting fluid by the zones of appreciable overburden thickness with a thick clayey column as shown in Figure 13.

The resistivity of the first layer in the study area is used to determine the soil corrosivity according to Tables 2–4.

The corrosivity ratings of the study area are classified as 26.5% slightly corrosive (SC) in the VES locations of V9-3, V8-3, V3-5, V5-4, V5-5, V4-3, V3-3, V2-3, and V1-2 where the resistivity of this first layer is between 60 and 180 $\Omega \cdot$m.

61.8% moderately corrosive (MC) in the VES locations of V6-1, V1-1, Sh11, Sh12, Sh13, V3-1, V3-2, V7-2, V7-3, V6-2, V10-4, V10-1, V9-2, V9-4, V8-2, V6-3, V5-3, V3-4, V2-1, V2-2, and V2-4 where the resistivity of this first layer is between 10 and 60 $\Omega \cdot$m.

Table 4 | Hydro-geophysical parameters of the studied 19 VES points, where no water samples are available

Location	*E* (UTM)	*N* (UTM)	*h (m)*	ρ_e ($\Omega \cdot m$)	ρ_w ($\Omega \cdot m$)	TR ($\Omega \cdot m^2$)	MTR ($\Omega \cdot m^2$)	EC (dS/m)	TDS (*ppm*)	*F*	*Ø (%)*	OPC (Ω^{-1})	Corr ($\Omega \cdot m$)
V10-4	376200	3969500	53.00	12.00	1.98	636.00	1,075.95	5.05	3,232.00	6.06	10.60	0.07	54.50
V10-3	375000	3970500	18.00	7.00	3.38	126.00	124.94	2.96	1,894.32	2.07	31.00	2.50	7.20
V10-1	372400	3972300	34.00	10.00	2.43	340.00	467.80	4.11	2,628.57	4.11	15.64	0.09	11.70
V10-2	373800	3971400	4.00	15.00	2.02	600.00	995.72	4.95	3,170.45	7.43	8.64	13.75	2.40
V9-1	371800	3971000	2.00	15.00	2.50	315.00	422.62	4.00	2,563.15	6.01	10.69	0.01	212.00
V9-2	373040	3970000	50.00	4.30	2.83	215.00	254.29	3.53	2,259.62	1.52	42.31	0.21	21.00
V9-4	375800	3968000	21.00	9.00	2.95	189.00	214.23	3.38	2,165.53	3.04	21.09	0.09	31.70
V8-2	372400	3968600	16.70	11.00	2.98	183.70	206.28	3.35	2,145.30	3.69	17.42	0.09	54.00
V6-3	371400	3963500	35.00	17.00	2.02	595.00	984.70	4.94	3,161.71	8.40	7.65	1.29	31.40
V5-3	367700	3963200	15.00	15.00	2.79	225.00	270.15	3.58	2,293.78	5.38	11.95	0.04	33.50
V5-5	370400	3961200	14.00	36.00	2.14	504.00	789.64	4.68	2,993.18	16.84	3.81	0.04	63.00
V4-3	368000	3960400	4.50	22.00	3.66	99.00	90.65	2.73	1,749.41	6.01	10.68	0.01	99.00
V3-3	367000	3958989	19.00	15.00	2.58	285.00	369.95	3.87	2,479.88	5.81	11.05	0.01	135.50
V3-4	368709	3957993	11.80	26.00	2.52	306.80	408.05	3.97	2,540.93	10.32	6.22	0.14	10.80
V2-1	364890	3958346	15.00	43.00	1.97	645.00	1,096.25	5.07	3,247.03	21.81	2.94	0.49	27.60
V2-2	366440	3957500	9.00	6.60	4.33	59.40	45.95	2.31	1,478.02	1.52	42.14	0.23	35.70
V2-3	367744	3956593	8.50	8.00	4.14	68.00	55.01	2.41	1,545.46	1.93	33.25	0.06	142.80
*V*2-4	369018	3955585	14.00	11.50	3.11	161.00	173.09	3.21	2,053.92	3.69	17.40	0.06	31.50
V1-2	367164	3954831	58.00	10.00	2.04	580.00	951.82	4.90	3,135.18	4.90	13.11	0.04	113.00

Table 5 | Dar-Zarrouk parameters of S, ρ_l, TR, ρ_t, and λ for the 34 VES points in the Khanasser Valley region, Syria

VES No	E (UTM)	N (UTM)	S (Ω^{-1})	ρ_l ($\Omega \cdot m$)	TR ($\Omega \cdot m^2$)	ρ_t ($\Omega \cdot m$)	λ
V6-1	368600	3965400	45.78	6.85	2,956.90	9.40	1.17
V9-3	374300	3969100	57.75	5.37	2,067.10	6.70	1.12
V2-5	370174	3954786	48.43	7.4	9,123.60	25.50	1.85
V1-1	365444	3955447	25.49	4.62	695.50	5.90	1.13
Sh11	372582	3963240	40.91	4.50	1,619.10	8.72	1.39
Sh12	372849	3964169	8.23	11.80	2,164.40	22.30	1.37
Sh13	374453	3967107	8.16	15.70	2,072.00	16.20	1.00
V8-3	373700	3967500	56.47	5.13	1,792.70	6.20	1.10
V3-1	364871	3960189	22.82	5.00	1,428.30	12.50	1.58
V3-2	365981	3959628	25.19	9.00	1,684.00	7.40	0.91
V7-2	370000	3967600	25.73	4.10	496.00	4.70	1.07
V7-3	371100	3966500	32.28	6.70	757.14	3.50	0.72
V3-5	370578	3956847	37.39	4.90	1,419.57	7.80	1.26
V5-4	369000	3962500	44.27	7.00	3,034.16	9.70	1.18
V6-2	369900	3964800	33.93	6.40	1,582.72	7.30	1.07
V10-4	376200	3969500	53.62	4.20	1,395.98	6.24	1.22
V10-3	375000	3970500	72.3	2.80	633.84	3.20	1.07
V10-1	372400	3972300	93.10	2.80	2,193.50	8.50	1.74
V10-2	373800	3971400	97.69	2.25	981.10	4.40	1.40
V9-1	371800	3971000	83.33	3.70	1,814.80	5.80	1.25
V9-2	373040	3970000	78.19	3.50	1,878.60	6.90	1.40
V9-4	375800	3968000	48.69	4.20	1,050.50	5.10	1.10
V8-2	372400	3968600	59.11	2.80	805.70	4.90	1.30
V6-3	371400	3963500	30.44	8.10	2,265.20	9.20	1.06
V5-3	367700	3963200	37.34	6.2	1,528.95	6.60	1.03
V5-5	370400	3961200	34.34	7.6	2,578.70	9.90	1.14
V4-3	368000	3960400	40.64	7.10	2,189.00	7.60	1.03
V3-3	367000	3958989	65.40	3.00	1,241.00	6.30	1.45
V3-4	368709	3957993	37.41	6.80	1,931.50	7.50	1.05
V2-1	364890	3958346	22.44	12.00	3,610.90	13.40	1.06
V2-2	366440	3957500	32.09	4.10	628.40	4.70	1.07
V2-3	367744	3956593	33.12	2.20	853.90	11.80	2.31
V2-4	369018	3955585	83.69	1.86	459.00	2.94	1.26
V1-2	367164	3954831	61.35	3.58	1,551.00	7.10	1.41

5.9% very strongly corrosive(VSC) in the VES locations of V10-3 and V10-2 where the resistivity of this first layer is less than 10 $\Omega \cdot m$, and 5.9% practically noncorrosive (PNC) in the VES locations of V2-5, and V9-1 where the resistivity of this first layer is bigger than 180 Ω m. The spatial variations of the corrosivity rating are shown in Figure 14.

The different information obtained through the Dar-Zarrouk geoelectrical parameters is highly important for the industries and for the locations of iron pipes to assuring the safeguarding of the hydrological setting for resident's safety in the study area. The suitable site locations for drilling boreholes must be selected in the regions with moderate/good protective capacity.

The methodology described in this paper is applied to a case study from the Khanasser Valley region. It is practiced for the first time in Syria for characterizing the Quaternary aquifer in the study region,

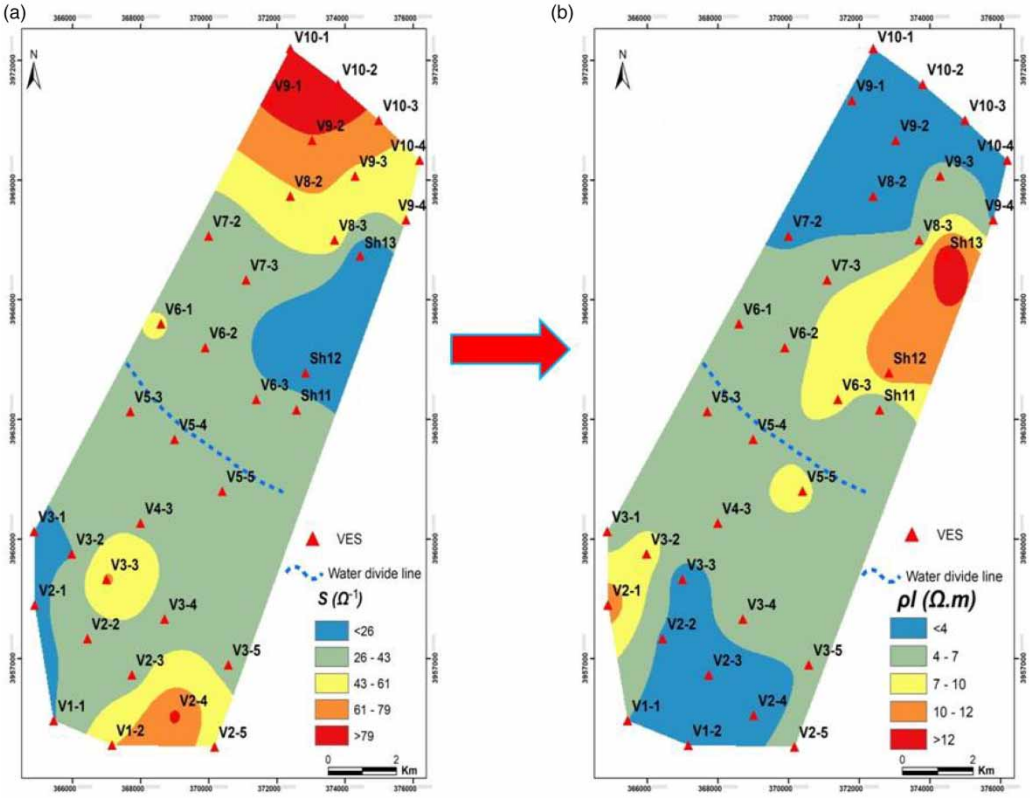

Figure 6 | (a) Spatial variations of S (Ω^{-1}) and (b) spatial variations of longitudinal resistivity ρ_l (Ω m).

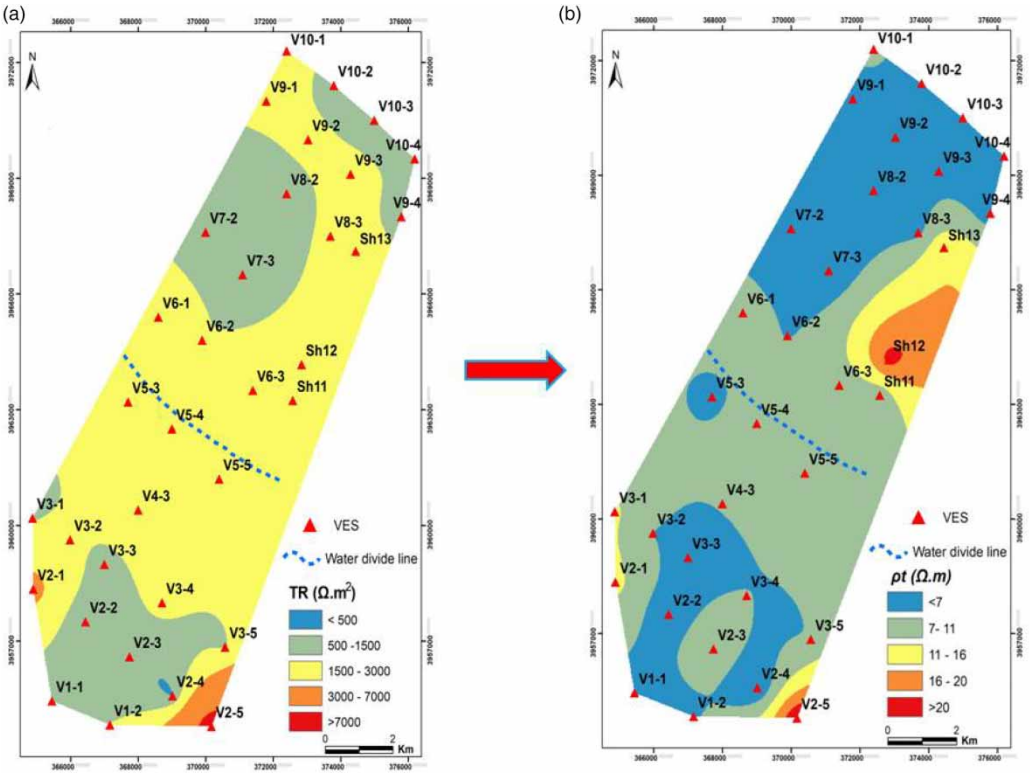

Figure 7 | (a) Spatial variations of TR (Ω m^2) and (b) spatial variations of transverse resistivity ρ_t (Ω m).

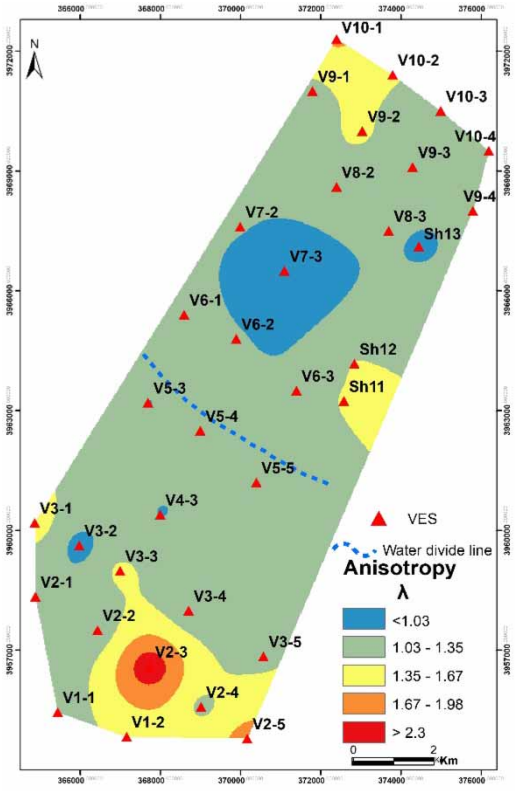

Figure 8 | Spatial variations of anisotropy coefficient (λ).

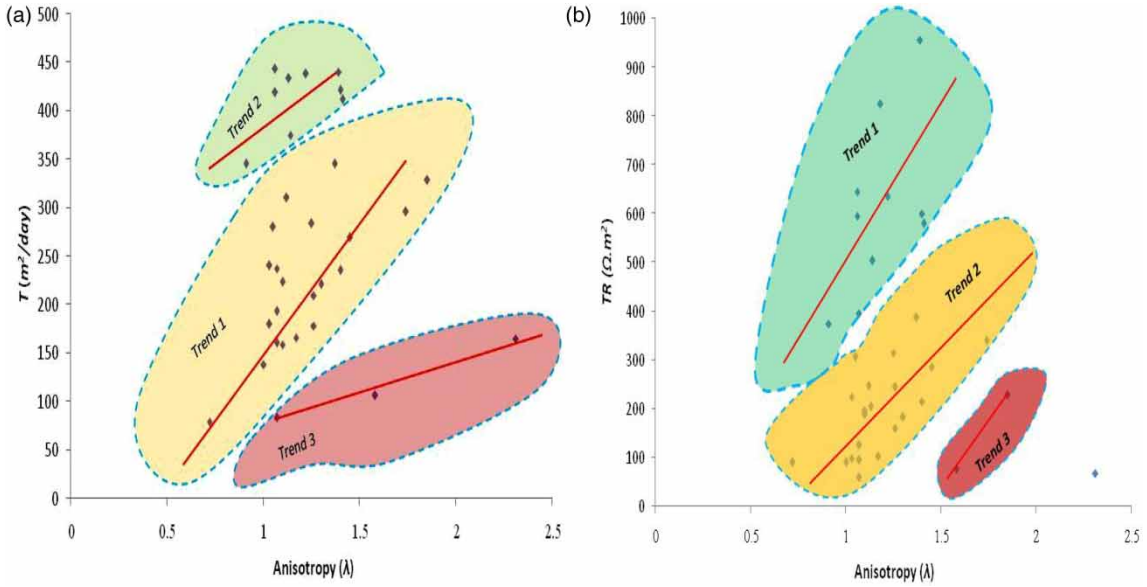

Figure 9 | (a) Three positive trends between anisotropy and shallow Quaternary aquifer transmissivity and (b) three positive trends between anisotropy and shallow Quaternary aquifer transverse resistance.

and can be easily transferred to cover and deal with different aquifers in the country. Its novelty and originality are proven, where it can be extended to other worldwide applications with different geological contexts.

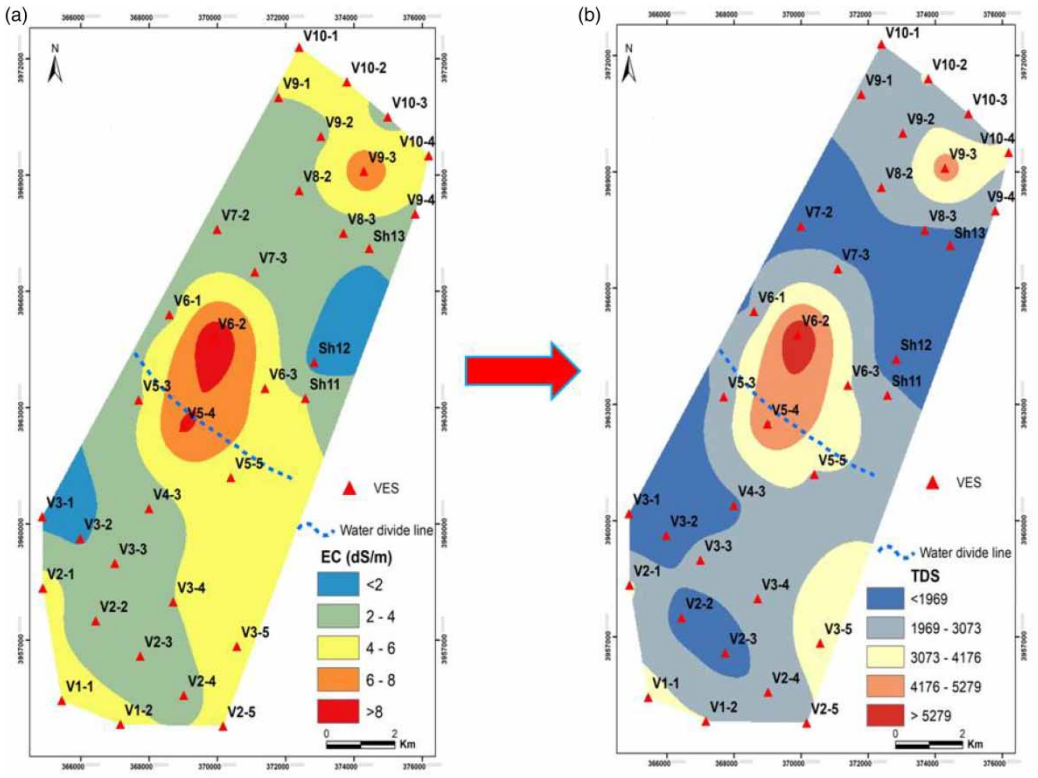

Figure 10 | (a) Spatial variations of EC (dS/m) and (b) spatial variations of TDS (ppm).

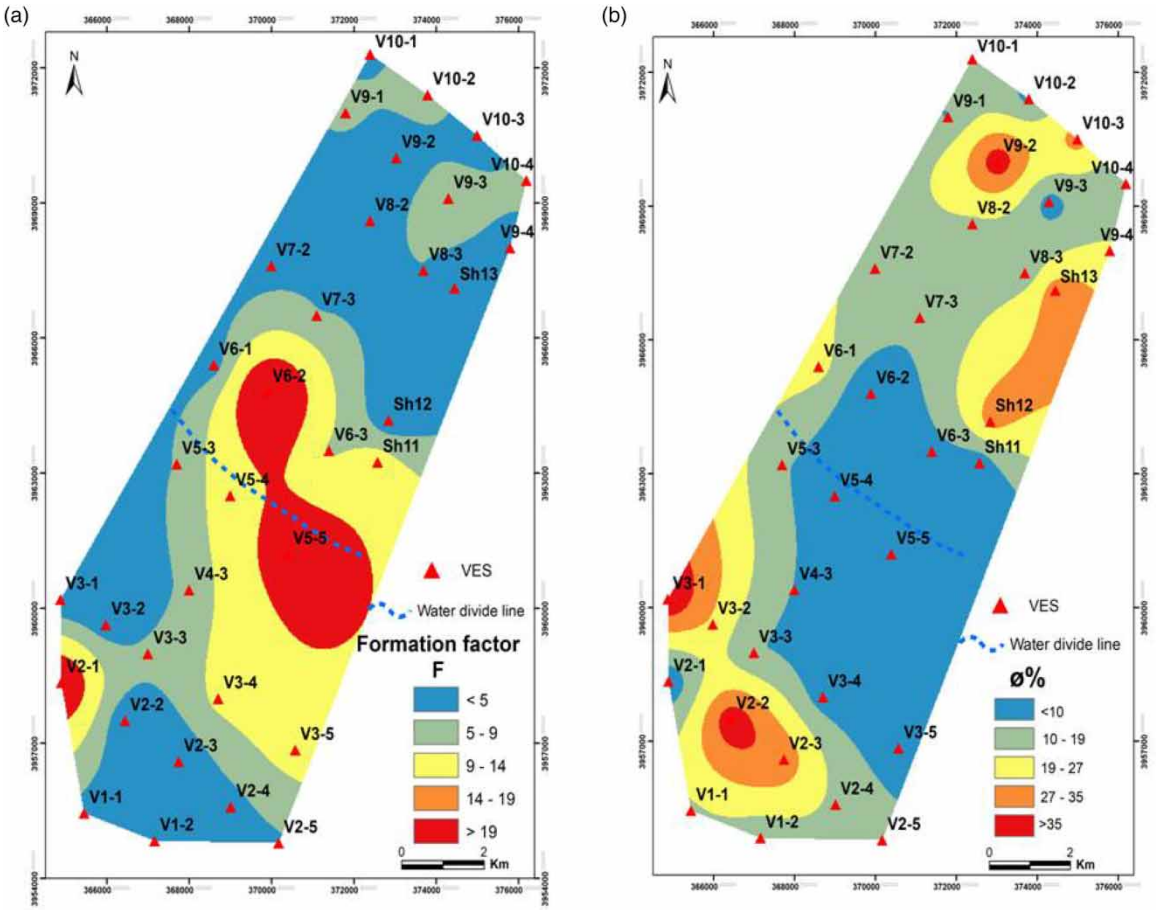

Figure 11 | (a) Spatial variations of *formation factor* (*F*) and (b) spatial variations of *porosity* (*Ø*%).

Table 6 | Geophysical and hydrological parameters at 34 VES points for Quaternary aquifer in the Khanasser Valley, Syria

	ρ_{rock} (Ω.m)	ρ_w (Ω.m)	h (m)	TR (Ω.m^2)	MTR (Ω.m^2)	EC (dS/m)	TDS (ppm)	F	(Ø%)	OPC (Ω^{-1})	Corr (Ω.m)
Min	4.30	1.00	4.50	59.40	37.66	1.30	86.00	1.50	2.80	0.01	2.40
Max	43.00	7.44	59.00	957.00	2,305.90	10.00	6,400.00	23.00	44.00	13.75	910.00
Average	15.10	3.00	22.30	313.30	492.00	4.10	2,592.00	6.50	16.90	0.94	77.00
SD	8.40	1.48	15.00	230.00	503.30	1.90	1,208.00	5.40	11.80	2.50	154.00

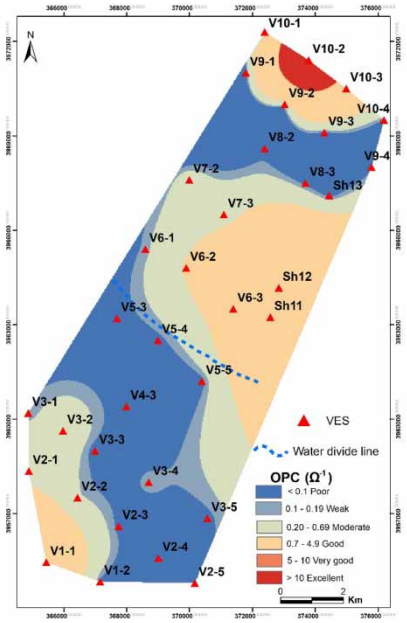

Figure 12 | OPC of the Quaternary aquifer in the Khanasser Valley.

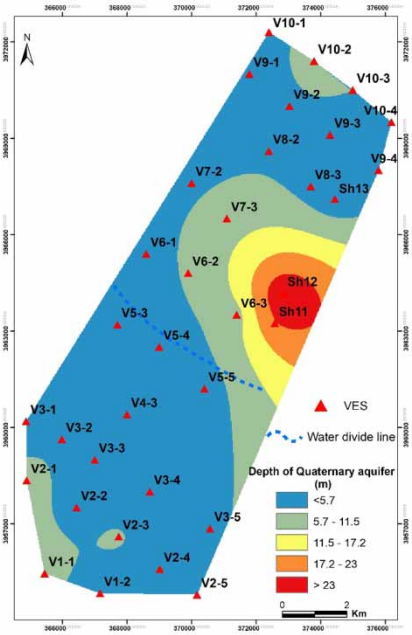

Figure 13 | Overburden thickness of the Quaternary aquifer in the Khanasser Valley.

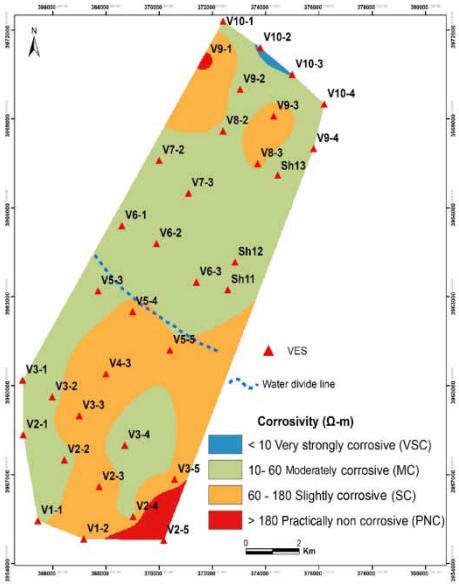

Figure 14 | Corrosion of the Quaternary aquifer in the Khanasser Valley.

6. CONCLUSION

The electrical resistivity (VES) technique is an efficient tool for most groundwater studies. It is used in this paper to investigate the characteristics of hydrogeological parameters of the Quaternary aquifer in the Khanasser Valley region, Northern Syria. An integrated methodology approach based on the DZPs is developed in this paper to investigate the parameters of EC, TDS, *F*, *Ø%*, TR, *S*, ρ_t, ρ_l, λ, OPC, and Corr. The calibrated empirical equation established between transverse resistance TR and the MTR allows us to extrapolate the values of the water resistivity in the VES locations where no water samples are available. This new calibration proceeding permits getting the EC, TDS, *F*, and the *Ø%* of the Quaternary aquifer in the entire study area. The management and modeling of water resources in the Khanasser Valley require such calibrated information.

The longitudinal conductance (DZP) is used to determine the OPC of the shallow Quaternary aquifer in the study area. The hydrological properties of the Quaternary aquifer and the protective capacity of a clayey aquifer overburden are also evaluated through the combination of aquifer layer thickness and resistivity using DZPs of transverse resistance and longitudinal conductance. The resistivity of the first layer is used to evaluate the corrosivity (Corr) in the study area.

This paper shows the importance of the electrical DZPs of transverse resistance, longitudinal conductance, and anisotropy in solving and obtaining the different constrained hydrogeological parameters. The integrated geoelectrical results obtained in this paper reasonably provide information on areas where industries can be sited, and iron pipes can be laid in order to safeguard the hydrological setting for resident's safety in the study area. Regions with moderate/good protective capacity are good sites for locating safe boreholes available for drinking water. The paper as designed through its specific useful methodology stimulates new insights and important environmental questions on the relations between aquifer depth and vulnerability of the water wells at certain depths, as a result of pollution related to the different human activities. It was also shown the importance of determining safe groundwater locations to get suitable drinking water in accordance with SDGs. One of the SDG is to ensure human health as regards water health and sanitation (WASH).

The novelty and the importance of the integrated methodology approach developed and applied in this paper are well proven and demonstrated at both industry and environmental levels. This new methodology approach can be therefore easily practiced and used worldwide in other similar geological contexts.

ACKNOWLEDGEMENTS

The author would like to thank Dr I. Othman, General Director of Syrian Atomic Energy Commission for permission to publish this research work. The German Ministry of Economic Cooperation and Development (BMZ) and German Agency for Technical Cooperation (GTZ) are acknowledged for financial and administrative

support to the Khanasser Valley Integrated Research Site (KVIRS) project. The late Professor Armin Rieser (coordinator of the project) from Bonn University, Germany is deeply thanked for many useful discussions during the preparation stages of this project.

ICARDA is highly thanked for providing the facilities and the logistics during the realization of the Khanasser Valley project. Dr Fares Asfari from *ICARDA* is cordially thanked for his many help during the different stages of the project. The two competent reviewers are cordially thanked for their professional critics, remarks, and suggestions that considerably improved the final version of this paper.

FUNDING

This work is part of an international scientific research under the No. 97-2001, which is totally funded by the authority of the Atomic Energy Commission of Syria.

HUMAN AND ANIMAL RIGHTS

This article does not contain studies with human or animal subjects.

DATA AVAILABILITY STATEMENT

All relevant data are included in the paper or its Supplementary Information.

CONFLICT OF INTEREST

The authors declare there is no conflict.

REFERENCES

Abdulrazzaq, Z. T., Agbasi, O. E., Alnaib, A. & Asfahani, J. 2023 Determining the optimum drilling sites for groundwater wells based on the hydro-geoelectrical parameters and weighted overlay approach via GIS in Salah Al-Din area, central Iraq. *Iranian Journal of Geophysics* **16**(4), 153–163. doi:10.30499/ijg.2022.324020.1401.

ACSAD. 1984 *Water Resources map of the Arab Countries*. The Arab Center for the Studies of Arid Zones and Dry Lands, Damascus, Syria.

Agunloye, O. 1984 Soil aggressivity along steel pipeline route at Ajaokuta southwestern Nigeria. *Journal of Minin and Geology* **121**, 97–10.

Akingboye, A. S. 2022 Geohydraulic characteristics and groundwater vulnerability assessment of tropically weathered and fractured gneissic aquifers using combined georesistivity and geostatistical methods. *Journal of the Nigerian Society of Physical Sciences* **4**, 497. https://doi.org/10.46481/jnsps.2022.497.

Akingboye, A. S., Bery, A. A., Kayode, J. S., Asulewon, A. M., Bello, R. & Agbasi, O. E. 2022 Near-surface crustal architecture and geohydrodynamics of the crystalline basement terrain of Araromi, Akungba-Akoko, SW Nigeria, derived from multi-geophysical methods. *Natural Resources Research* **31**(1), 215–236. https://doi.org/10.1007/s11053-021-10000-z.

Archie, E. 1942 The electrical resistivity log as an aid in determining some reservoir characterestics. Technical Publication 1422, Petroleum Technology. American Institute of Mining and Metallurgical Engineer, New York, USA; 8.

Aretouyap, Z., Asfahani, J., Abdulrazzaq, Z. T. & Tchato, S. C. 2022 Contribution of the fuzzy algebraic model to the sustainable management of groundwater resources in the Adamawa watershed. *Journal of Hydrology: Regional Studies* **43**, 101198. https://doi.org/10.1016/j.ejrh.2022.101198.

Asfahani, J. 2007 Electrical Earth Resistivity surveying for delineating the characteristics of groundwater in semiaridregion in Khanaser Valley, Northern Syria. *Hydrological Processes* **21**, 1085–1097.

Asfahani, J. 2013 Groundwater potential estimation using vertical electrical sounding measurements in the semi-arid Khanasser Valley region, Syria. *Hydrological Sciences Journal – Journal des Sciences Hydrologiques*. http://dx.doi.org/10.1080/02626667.2012.751109.

Asfahani, J. 2016 Hydraulic parameters estimation by using an approach based on verticalelectrical soundings (VES) in the semi-arid Khanasser valley region, Syria. *J. Afr. Earth Sci.* **117**, 196–206. doi:10.1016/j.jafrearsci.2016.01.018.

Asfahani, J. 2021 Classification of the transmissivity spatial variations of Quaternary aquifer in the semi-arid Region Khanasser Valley, Northern Syria. *Journal of African Earth Sciences* **182**, 104269. https://doi.org/10.1016/j.jafrearsci.2021.104269.

Asfahani, J. & Abou Zakhem, B. 2013 Geoelectrical and hydrochemical investigations for characterizing the salt water intrusion in the KhanasserValley, Northern Syria. *Acta Geophysica* **61**(2), 422–444. doi:10.2478/s11600-012-0071-3.

Baeckman, W. V. & Schwenk, W. 1975 *Handbook of Cathodic Protection: The Theory and Practice of Electrochemical Corrosion Protection Techniques*. Press, Redhill.

Barker, R., Rao, T. V. & Thangarajan, M. 2001 Delineation of contaminant zone through electrical imaging technique. *Curr. Sci.* **81**(3), 277–283.

Bayewua, O. O., Oloruntolab, M. O., Mosuroa, G. O., Laniyana, T. A., Ariyoa, S. O. & Fatoba, J. O. 2018 Assessment of groundwater prospect and aquifer protective capacity using resistivity method in Olabisi Onabanjo University campus, Ago-Iwoye, South western Nigeria. *NRIAG J Astron Geophys* **7**, 347–360.

de Almeida, A., Maciel, D. F., Sousa, K. F., Nascimento, C. T. C. & Koide, S. 2021 Vertical electrical sounding (VES) for estimation of hydraulic parameters in the porous aquifer. *Water* **13**, 170. https://doi.org/10.3390/w13020170.

Flathe, H. 1955 Possibilities and limitations in applying geoelectrical methods to hydrogeological problems in the coastal area of northwest Germany. *Geophysical Prospecting* **3**, 95–110.

Freeze, R. A. & Cheery, J. A. 1979 *Groundwater*. Prentice-Hall Inc, Englewood, Cliffs, p. 604.

George, N. J., Ibanga, J. I. & Ubom, A. I. 2015 Geoelectro hydrogeological indices of evidence of ingress of saline water into freshwater in parts of coastal aquifers of Ikot Abasi, Southern Nigeria. *Journal of African Earth Sciences* **109**, 37–46.

George, N. J., Akpan, A. E. & Ekanem, A. M. 2016 Assessment of textural variational pattern and electrical conduction of economic and accessible quaternary hydrolithofacies via geoelectric and laboratory methods in SE Nigeria: a case study of select locations in Akwa Ibom State. *Journal of Geological Society of India* **88**(4), 517–528. doi:10.1007/s12594-016-0514-6.

Hasan, M., Shang, Y., Jin, W. & Akhter, G. 2019 Assessment of aquifer vulnerability using integrated geophysical approach in weathered terrains of south China. *Open Geosciences* **11**(1), 1129–1150. https://doi.org/10.1515/geo-2019-0087.

Hasan, M., Shang, Y., Jin, W. & Akhter, G. 2021 Estimation of hydraulic parameters in a hard rock aquifer using integrated surface geoelectrical method and pumping test data in southeast Guangdong, China. *Geosciences Journal* **25**(2), 223–242. https://doi.org/10.1007/s12303-020-0018-7.

Henriet, J. P. 1976 Direct application of Dar-Zarrouk parameters in groundwater survey. *Geophys. Prospect.* **24**, 344–353.

Ibuot, J. C., Okeke, F. N., George, N. J. & Obiora, D. N. 2017 Geophysical and physicochemical characterization of organic waste contaminationof hydrolithofacies in the coastal dumpsite of AkwaIbomState, Southern Nigeria. *Water SciTechnol Water Supply* **17**(6), 1626–1637.

Ikpe, E. O., Ekanem, A. M. & George, N. J. 2022 Modelling and assessing the protectivity of hydrogeological units using primary and secondary geoelectric indices: a case study of Ikot Ekpene Urban and its environs, southern Nigeria. *Modeling Earth Systems and Environment*. https://doi.org/10.1007/s40808-022-01366-x.

Keller, G. V., 1987 Rock and mineral properties. In: *Electromagnetic Methods in Applied Geophysics: Part A*, (Nabighian, M. C., ed.). Tulsa, pp. 13–52. Tulsa, OK: Society of Exploration Geophysicists.

Keswick, B. H., Wang, D. & Gerba, C. P. 1982 The use of microorganisms as groundwater tracers – A review. *Groundwater.* **20**(2), 142–149.

Maillet, R. 1974 The fundamental equations of electrical prospecting. *Geophy* **1974**(12), 529–556.

Mogaji, K. A., Adiat, K. A. N. & Oladapo, M. I. 2007 Geoelectric investigation of the dape phase III housing estate F.C.T Abuja, north–central Nigeria. *J. Earth Sci.* **1**(2), 76–84.

Obiora, N. O., Adeolu, E. & Ibuot, J. C. 2015a Evaluation of aquifer protective capacity of overburden unit and soil corrosivity in Makurdi, Benue State, Nigeria, using electrical resistivity method. *Journal of Earth System Sciences* **124**(1), 125–135.

Obiora, D. N., Ibuot, J. C. & George, N. J. 2015b Evaluation of aquifer potential, geoelectric and hydraulic parameters in Ezza North, southeastern Nigeria, using geoelectric sounding. *Int J Sci Technol*. https:// doi.org/ 10.1007/ s13762- 015- 0886-y.

Oguama, B. E., Ibuot, J. C., Obiora, D. N. & Aka, M. U. 2019 Geophysical investigation of groundwater potential, aquifer parameters, and vulnerability: a case study of Enugu State College of Education (Technical). *Model Earth Syst Environ* **5**, 1123–1133. https://doi.org/10.1007/s4080 8-019-00595–x.

Oladapo, M. I. & Akintorinwa, O. J. 2007 Hydrogeophysical study of Ogbess Southwestern Nigeria. *Glob J Pure Appl Sci* **13**(1), 55–61.

Oladapo, M. I., Mohammed, M. Z., Adeoye, O. O. & Adetola, O. O. 2004 Geoelectric investigation of the Ondo-State housing corporation estate ijapoAkure southwestern Nigeria. *Journal of Mining and Geology* **40**, 41–48.

Omoyoloye, N. A., Oladapo, M. I. & Adeoye, O. O. 2008 Engineering geophysical study of adagbakuja newtown development southwestern Nigeria. *Journal of Earth Science* **2**(2), 55–63.

Orellana, E. & Mooney, H. M. 1966 *Master Tables and Curves for Vertical Electrical Sounding Over Layered Structures*. interciencia, Madrid, Spain.

Ponikarov, V. P. 1964 *The Geological Map of Syria, 1:200.000 and Explanatory Notes*. SyrianArabRepublic, Ministry of Industry, Department of Geological and Mineral Research, Damascus, Syria.

Reilly, T., Dennehy, K. F., Alley, W. M. & Cunningham, W. L. 2008 *Groundwater Availability in the United States*. US Geological Society Circular, 1323. US Geological Survey, Reston, VA.

Schweers, W., Rieser, A., Bruggeman, A., Abu-Zakhem, B., Asfahani, J., Kadkoy, N. & Kasmo, B. 2002 Assessment of groundwater resources for sustainable management in the Khanasser valley, northwest Syria. In: *Paper Presented at ACSAD/BGR Workshop on Soil and Groundwater Quality: Monitoring Management and Protection*, 23–25 June 2002, Amman.

Umar, N. D. & Igwe, O. 2019 Geo-electric method applied to groundwater protection of a granular sandstone aquifer. *Appl Water Sci* **9**, 112. https://doi.org/10.1007/s13201-019-0980-2.

Van Stempvoort, D. V., Ewert, L. & Wassenaar, L. 2013 Aquifer vulnerability index: a gis – compatible method for groundwater vulnerability mapping. *Can Water Resour J Revue Canadienne des Resources Hydriques* **18**(1), 25–37.

Velpen, B. A. 2004 *Win RESIST Version 1.0. MSc Research Project*, ITC, Deft, Netherlands.

Yahaya, M. I., Mohammed, S. & Seasonal, B. K. 2009 Variation of heavy metals concentration in Abattoir dumpsite soil in Nigeria. *Journal of Applied Science and Environmental Management* **13**(4), 9–13.

Zohdy, A. A. R. 1989 A new method for the automatic interpretation of Schlumberger and Wenner sounding curves. *Geophysics* **54**, 245–253.

Zohdy, A. A. R. & Bisdorf, R. J. 1989 *Schlumberger Sounding Data Processing and Interpretation Program*. U.S. Geological Survey, Denver.

Zohdy, A. A. R., Eaton, G. P. & Mabey, D. R. 1974 *Application of Surface Geophysics to Groundwater Investigations*. U.S. Geological, Survey.

First received 14 March 2023; accepted in revised form 6 May 2023. Available online 17 June 2023